Vibronic Coupling and Jahn−Teller Effects in Negatively Charged Corannulene

Tokio Yamabe, Kazuyuki Yahara, Takashi Kato, and Kazunari Yoshizawa*

Department of Molecular Engineering, Kyoto University, Sakyo-ku, Kyoto 606-8501, Japan, and Institute for Fundamental Chemistry, 34-4 Takano-Nishihiraki-cho, Sakyo-ku, Kyoto 606-8103, Japan

Received: July 20, 1999; In Final Form: November 16, 1999

The vibronic (vibrational−electronic) interactions and the Jahn−Teller distortions in the mono- and trianions of corannulene, which shows a bowl-shaped C_{5v} structure in the neutral state, are discussed. Jahn−Teller active E_2 modes of vibration remove the degenerate E_1 state of the mono- and trianions to lead to C_s structures. We calculate the linear vibronic coupling constants in the corannulene anions using the B3LYP method, a hybrid (Hartree−Fock/density functional theory) method. The lowest two vibrational modes of 142 and 282 cm^{-1} have large vibronic coupling constants, thus significantly contributing to the Jahn−Teller distortions. The electronic features of corannulene and coronene are discussed from a viewpoint that corannulene can be viewed as a fragment of C_{60} and coronene as a fragment of graphite. Computed vibronic coupling constants in the corannulene anions are much larger than those in the coronene anions. The atomic motion in the Jahn−Teller active E_2 modes of corannulene is somewhat vertical to the bowl-shaped structure. On the other hand, the Jahn−Teller active E_{2g} modes of coronene and the resultant molecular distortions in its anions are strictly fixed on the molecular plane by symmetry. This contrast can explain the different vibronic features in corannulene and coronene. This fact may characterize the high-T_c superconductivity over 30 K in the alkali−metal complexes of C_{60} and the low-T_c superconductivity in the graphite intercalation compounds.

Introduction

The first synthesis of corannulene $C_{20}H_{10}$ (**1**) was reported by Barth and Lawton in 1966.[1] Molecular orbital calculations were applied to the corannulene system immediately after the synthesis.[2] An X-ray diffraction measurement confirmed that this molecule has a bowl-shaped structure with C_{5v} symmetry and that the five six-membered rings in the periphery are significantly out of plane.[3] After the development of new synthetic strategies,[4] many researchers have extensively studied this bowl-shaped hydrocarbon taking cognizance of the C_{60} fullerene (**2**).[5,6] Unique structural and electronic properties in this molecule have recently been characterized. First, corannulene is so flexible that it undergoes rapid bowl-to-bowl inversion in solution as evidenced by the dynamic NMR behavior of several derivatives.[4b] Second, the reduction of corannulene up to the tetraanion is possible as observed by parallel detection of optical absorption, electron spin resonance (ESR), and NMR spectroscopies.[7] Ab initio[8] and semiempirical[9] molecular orbital calculations on the neutral and anionic states of corannulene were carried out, concerning the geometry, the inversion barrier, and the vibrational structure (Chart 1).

One of the reasons that many researchers have had special interests in bowl-shaped carbon materials is, of course, because of the brilliant discovery of the superconductivity in the alkali-doped A_3C_{60} complexes,[10] which was later found to exhibit high superconductive transition temperatures (T_c values) of more than 30 K[11] and of 40 K under pressure.[12] A large amount of theoretical work on the vibronic coupling of the fullerene complexes was carried out by Varma et al.,[13] Lannoo et al.,[14] and other groups[15] to account for the interesting superconductive phenomena of the A_3C_{60} complexes. Because of the highly symmetric structure with I_h symmetry, certain Jahn−Teller[16] distortions are expected to occur in order to lift the degeneracy of the 3-fold degenerate lowest unoccupied molecular orbital (LUMO). Because corannulene has a highly symmetric C_{5v} structure, it has the 2-fold degenerate highest occupied molecular orbital (HOMO) and the 2-fold degenerate LUMO, both having an e_1 label of symmetry. We therefore expect that similar Jahn−Teller distortions should occur in negatively charged corannulene.

CHART 1

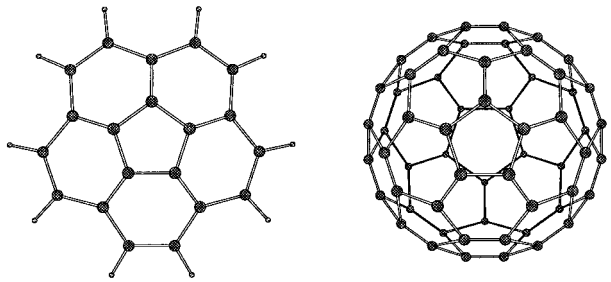

1 **2**

The graphite intercalation compounds (GICs) exhibit superconductivity,[17] but in contrast to the A_3C_{60} complexes the T_c values of the GICs are low, the highest transition temperature being 5.5 K in C_4K.[18,19] The reader can refer to useful discussions on the superconductivity of the GICs in a review paper.[20] It is important to consider why the A_3C_{60} complexes show high T_c values. The remarkable contrast between the high-T_c superconductivity of the A_3C_{60} complexes and the low-T_c superconductivity of the GICs can be derived from the fact that the C_{60} molecule involves a bowl-shaped structure but the graphite sheet is planar. The discussion of Haddon[21] on the rehybridization of the π-orbitals and the 2s atomic orbital may

* To whom correspondence should be addressed (E-mail: kazunari@scl.kyoto-u.ac.jp).

10.1021/jp992496g CCC: $19.00
Published on Web 01/05/2000

be useful for the understanding of the high-T_c superconductivity of the A_3C_{60} complexes. However, Devos and Lannoo[22] recently calculated electron−phonon coupling constants of a series of aromatic hydrocarbons including corannulene and coronene, showing that the coupling constants are independent of the curvature of aromatic hydrocarbons and inversely proportional to the number of carbon atoms.

In our previous work, we analyzed the vibronic interactions and the Jahn−Teller distortions in charged benzene, [18]-annulene,[23] [30]annulene,[24] coronene,[25] and the $(SiH)_{20}$ and $(SiH)_{24}$ clusters.[26] We also discussed the electron−phonon interactions in charged [18]annulene[27] and C_{36}[28] and their role in possible superconductivity. The purpose of this paper is to investigate the vibronic coupling and the Jahn−Teller distortions in the corannulene anions. It is quite interesting to characterize the electronic features of corannulene and coronene in that corannulene and coronene can be viewed as fragments of C_{60} and graphite, respectively. We discuss how the structural difference between corannulene and coronene affects the vibronic interactions in these hydrocarbon anions.

Theoretical Background

Here we summarize a theoretical background for the Jahn−Teller effects in degenerate molecules discussed in previous papers.[23−25] Because corannulene has the 2-fold degenerate HOMO (e_1) and LUMO (e_1), the electronic states of its mono- and trianions are unstable and thus Jahn−Teller distortions would take place. In this paper we focus upon the diagonal processes that can couple the electronic states that belong to the same irreducible representations. Thus, the symmetry of the Jahn−Teller active modes can be determined from the direct product of the E_1 electronic state of the mono- and trianions as follows:

$$E_1 \times E_1 = A_1 + A_2 + E_2 \tag{1}$$

Here we consider that only the vibronic coupling between the E_1 electronic state and the E_2 vibrational modes should be essential because both A_1 and A_2 vibrational modes retain the 5-fold axis and consequently it can hardly couple with this degenerate electronic state. The normal modes of vibration for corannulene are distributed into the symmetry species, as indicated below:

$$\Gamma_{vib} = 9A_1 + 7A_2 + 16E_1 + 18E_2 \tag{2}$$

The number of the 2-fold degenerate Jahn−Teller active E_2 modes is 18, and therefore multimode problems must be considered in this case. However, in the limit of linear vibronic coupling one can treat each vibrational mode independently.[29]

The dimensionless linear vibronic coupling constant[13−15] of the mth vibrational mode in the mono- and trianions can be defined by

$$g_{E_2m} = \frac{1}{2\hbar\omega_m}\left\langle E_1 \left\| \left(\frac{\partial V_{E_2m}}{\partial q_{E_2m}}\right)_0 \right\| E_1 \right\rangle \qquad (m = 1,2,\cdots,18) \tag{3}$$

where q_{E_2m} is the dimensionless normal coordinate[30] of the mth vibrational mode and this is expressed by using the normal coordinate Q_{E_2m} as

$$q_{E_2m} = \sqrt{\omega_m/\hbar}\,Q_{E_2m} \qquad (m = 1,2,\cdots,18) \tag{4}$$

and V_{E_2m} is the Jahn−Teller coupling matrix of the mth mode in the mono- and trianions defined as

$$V_{E_2m} = A_m \begin{pmatrix} -Q_{E_2\epsilon m} & Q_{E_2\theta m} \\ Q_{E_2\theta m} & Q_{E_2\epsilon m} \end{pmatrix} \qquad (m = 1,2,\cdots,18) \tag{5}$$

Here A_m is the reduced matrix element and is the slope in the original point (i.e., $Q_{E_2\epsilon m} = Q_{E_2\theta m} = 0$) on the potential energy surface, the so-called Mexican hat, along each vibrational mode. This is defined as

$$A_m = \frac{1}{2}\left\langle E_1 \left\| \left(\frac{\partial V_{E_2m}}{\partial Q_{E_2m}}\right)_0 \right\| E_1 \right\rangle \qquad (m = 1,2,\cdots,18) \tag{6}$$

In this paper, we performed vibrational analyses in the neutral state under C_{5v} symmetry while energetical single-point calculations for the A_m values were performed in the mono- and trianions. That is, we calculate the first-order derivatives on the surface of the corannulene anions along the normal coordinate directions in the neutral corannulene.

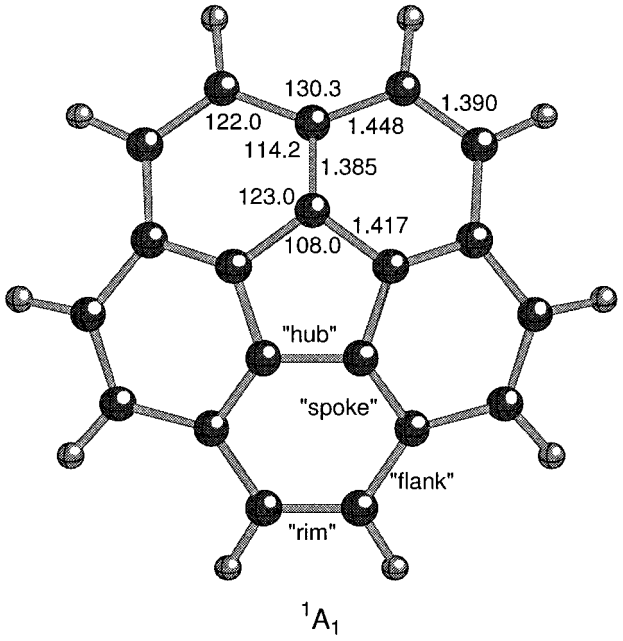

Figure 1. An optimized C_{5v} structure of corannulene at the B3LYP/6-31G* level.

Results and Discussion

Electronic Structure of Corannulene. The structure of neutral corannulene was optimized under C_{5v} symmetry using the hybrid density-functional theory (DFT) method of Becke[31] and Lee, Yang, and Parr[32] (B3LYP) and the 6-31G* basis set.[33] GAUSSIAN 94 program package[34] was used for our theoretical analyses. This level of theory is, in our experience, sufficient for reasonable descriptions of the geometric, electronic, and vibrational structures of hydrocarbons. An optimized C_{5v} structure of neutral corannulene is shown in Figure 1. There is a distinct variation in the C−C distances. The shortest "spoke" bond is 1.385 Å, the "rim" and "hub" bonds are 1.390 and 1.417 Å, respectively, and the longest "flank" bond is 1.448 Å. Because the distances of the spoke, rim, hub, and flank bonds determined from an X-ray structural analysis[3] are 1.391(4), 1.402(5), 1.413(3), and 1.440(2) Å, respectively, the B3LYP-optimized structure is in excellent agreement with the structure determined from the X-ray analysis. We can rationalize these geometrical features from a close inspection of the HOMO

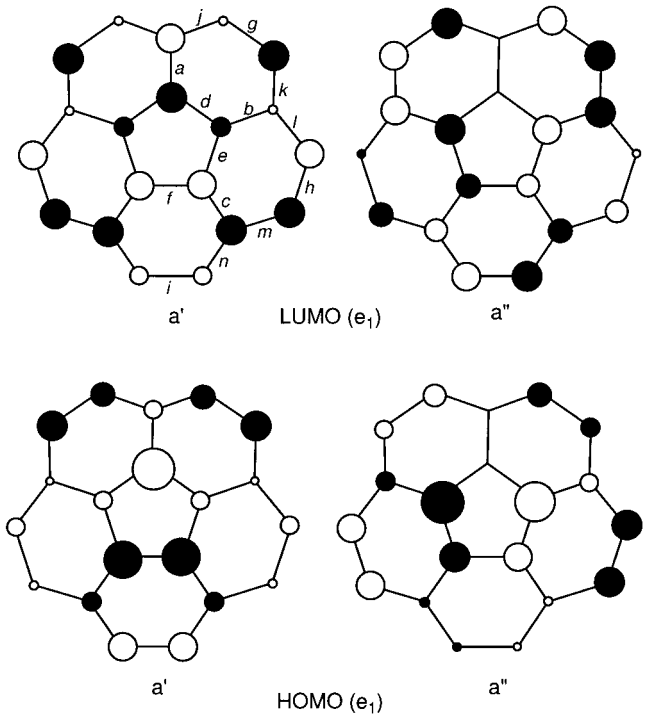

Figure 2. The HOMO and the LUMO of corannulene. Symmetry labels under C_{5v} and C_s symmetry are indicated.

shown in Figure 2. The atomic orbitals between the two carbon atoms forming a spoke are coupled in phase. This orbital nature is consistent with the fact that the spoke bonds are shorter than other C−C bonds. In a similar fashion, we can explain why the flank bonds are longer than others in view of the HOMO, in which the atomic orbitals between the two carbon atoms that form a flank are combined out of phase. Calculated relative bowl depth defined by the distance from the best plane of the five carbon atoms of the central hubs to the best plane of the 10 carbon atoms in the rims is 0.86 Å. According to the X-ray structural analysis,[3] the relative bowl depth of corannulene is 0.89 Å, thus our B3LYP geometry is again in good agreement with the experimental result. It is interesting to compare the geometries of corannulene and coronene.[25] In contrast to corannulene, the rim of coronene is very short (1.372 Å), due to the character of the HOMO in which the atomic orbitals between the two carbon atoms forming a rim are in phase.

The electron affinity in the monoanion was computed to be 0.05 eV. As mentioned earlier, corannulene can be easily reduced electrochemically leading to charge-transfer complexes with alkali metals such as lithium and potassium, and NMR measurements showed that the tetraanion is the final reduction product of corannulene in solution.[7] The reason that corannulene is successfully reduced up to the tetraanionic state can be explained by the low-lying LUMO of −1.57 eV at the B3LYP/6-31G* level, which is slightly below the LUMO of coronene (−1.41 eV).

Vibronic Interactions in the Corannulene Anions. Our knowledge of the vibrational structure of corannulene is rather limited. IR absorption bands were observed at 840, 905, 1135, 1310, 1430, 3010, and 3050 cm^{-1},[1,1b] and theoretical vibrational analyses were carried out at the MNDO and the Hartree−Fock/6-31G* levels of theory.[9a,8d] These Hartree−Fock methods tend to overestimate experimental values by ca. 10%. The B3LYP method can nicely reproduce the vibrational frequencies of aromatic hydrocarbons; for example, calculated wavenumbers of benzene are accurate within a range of 2.5−4%.[23] We performed a vibrational analysis of neutral corannulene with quadratic force constants, which are the second derivatives of the potential energy with respect to mass-weighted Cartesian displacements. A complete set of calculated vibrational frequencies is listed in Table 1. The computed vibrational frequencies of the 84 vibrational modes of eq 2 are all real, which confirms that this C_{5v} structure is at least a local energy minimum on the potential energy surface. It is in fact the global minimum point. Computed Jahn−Teller active E_2 modes of vibration (ω_m) are shown in Figure 3. It is essential to note that the atomic motion in some of these Jahn−Teller active modes is somewhat vertical to the bowl-shaped structure.

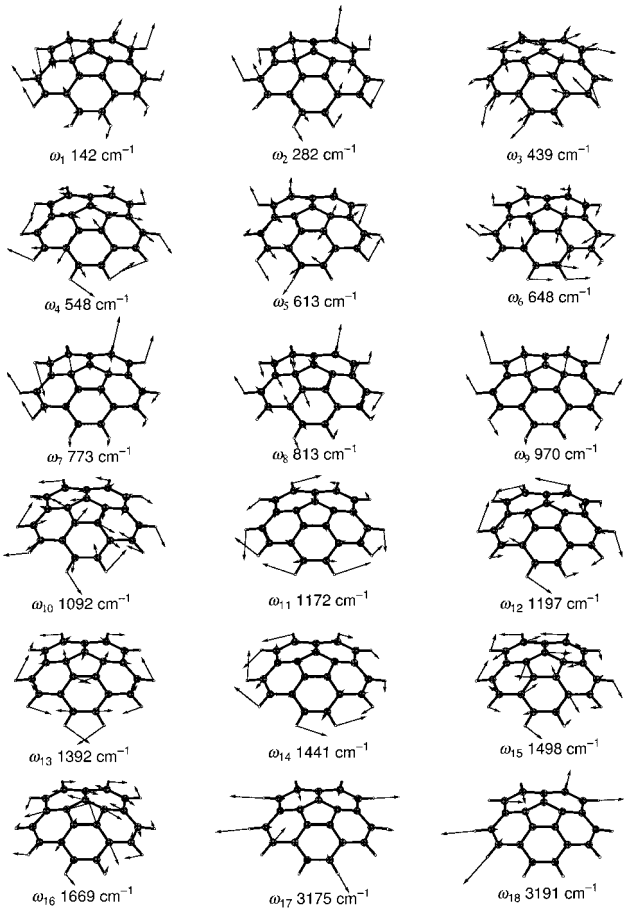

Figure 3. E_2 vibrational modes of corannulene.

In the corannulene anions, certain Jahn−Teller distortions are expected to occur. We calculated first-order derivatives (A_m of eq 6) at the point $Q_{E_2\epsilon m} = Q_{E_2\theta m} = 0$ on the potential energy surface of the corannulene anions by distorting the molecule along each E_2 normal coordinate indicated in Figure 3. We can

TABLE 1: Calculated Vibrational Frequencies of Neutral Corannulene with C_{5v} Symmetry

symmetry label	wavenumber (cm^{-1})
A_1	142, 560, 606, 857, 1052, 1270, 1481, 1672, 3193
A_2	542, 650, 937, 954, 1245, 1527, 3173
E_1	313, 410, 453, 673, 760, 834, 870, 961, 1172, 1224, 1343, 1459, 1486, 1670, 3174, 3192
E_2	142, 282, 439, 548, 613, 648, 773, 813, 970, 1092, 1172, 1197, 1392, 1441, 1498, 1669, 3175, 3191

TABLE 2: Calculated Reduced Masses of E_2 Modes of Neutral Corannulene and Computed Vibronic Constants (g_{E_2m}) in the Mono- and Trianions of Corannulene

mode (cm^{-1})	ω_1 (142)	ω_2 (282)	ω_3 (439)	ω_4 (548)	ω_5 (613)	ω_6 (648)	ω_7 (773)	ω_8 (813)	ω_9 (970)	ω_{10} (1092)	ω_{11} (1172)	ω_{12} (1197)	ω_{13} (1392)	ω_{14} (1441)	ω_{15} (1498)	ω_{16} (1669)	ω_{17} (3175)	ω_{18} (3191)
red. masses	4.43	4.33	7.89	4.26	4.81	6.17	1.35	7.66	1.30	4.75	1.49	3.29	3.96	1.65	7.32	9.53	1.09	1.09
$g_{E_2m}(-1)$	2.11	1.08	0.55	0.38	0.71	0.18	0.04	0.10	0.30	0.16	0.24	0.17	0.13	0.19	0.22	0.41	0.03	0.04
$g_{E_2m}(-3)$	1.43	2.23	0.91	0.28	0.67	0.42	0.21	0.23	0.27	0.14	0.19	0.29	0.08	0.28	0.44	0.30	0.02	0.02

thus evaluate dimensionless linear vibronic coupling constants g_{E_2m} from computed A_m values by using eqs 3, 4, and 6. Computed reduced masses of the E_2 modes and dimensionless linear vibronic coupling constants for the anions are listed in Table 2.

Let us first examine the vibronic coupling constants for the monoanion. As seen from this table, the coupling constants in the lowest two E_2 modes of 142 cm^{-1} (ω_1) and 282 cm^{-1} (ω_2) are very large; thus the two modes should play an important role in the Jahn−Teller distortions. In addition to these remarkable vibrational modes, the 439 cm^{-1} (ω_3) and 613 cm^{-1} (ω_5) modes also give relatively large coupling constants. In the high-frequency region, however, only the 1669 cm^{-1} (ω_{16}) mode has a large coupling constant. This is a C−C stretching mode and the reduced mass of this mode is the largest (9.53), which shows that the motion of carbon atoms is dominant in this mode. Similar conclusions can be derived for the trianion. As in the monoanion, the lowest two E_2 modes have very large coupling constants in the trianion. The other low-frequency modes of 439 cm^{-1} (ω_3) and 613 cm^{-1} (ω_5) also have relatively large coupling constants. In the high-frequency region, however, the 1498 cm^{-1} (ω_{15}) mode has a large coupling constant. We can thus conclude that the lowest two E_2 modes should extensively contribute to the Jahn−Teller distortions in the mono- and trianions of corannulene.

Jahn−Teller Distortions in Negatively Charged Corannulene. Next we performed geometry optimizations for the corannulene anions. According to the epikernel principle,[36] we can predict that the C_{5v} structure should be distorted into C_s structures by the Jahn−Teller active E_2 modes indicated in Figure 3. Structures of the mono- and trianions optimized under C_s symmetry are presented in Figure 4. The HOMO and the LUMO of e_1 label under C_{5v} symmetry are split into a′ and a″ under C_s symmetry, as indicated in Figure 2. According to our calculations, the ^{2}A′ state is only 0.007 kcal/mol more stable than the ^{2}A″ state in the monoanion, and the ^{2}A′ state is only 0.003 kcal/mol less stable than the ^{2}A″ state in the trianion. Thus, the two states have nearly equal total energies in both anions, as expected. We can see that the structures of these anions are significantly deformed, some C−C bonds being increased and others decreased by electron doping. These features are examined in detail in Table 3 and computed C−C bond lengths in the neutral, monoanionic, and trianionic states are summarized. The values in parentheses signify the changes in bond length by electron doping.

These geometrical changes are reasonable in view of the phase patterns of the LUMO indicated in Figure 2. Let us examine in detail the geometrical changes induced by electron doping. For example, all of the spoke bonds are stretched by electron doping because the atomic orbitals between the two carbon atoms forming a spoke are combined out of phase in both a′ and a″ LUMOs. The spoke bonds of the trianion are much longer than those of the monoanion because putting three electrons in the degenerate LUMO should drive a molecular distortion which is larger than that driven by one electron. The changes of the C−C distances in the flank bonds are also

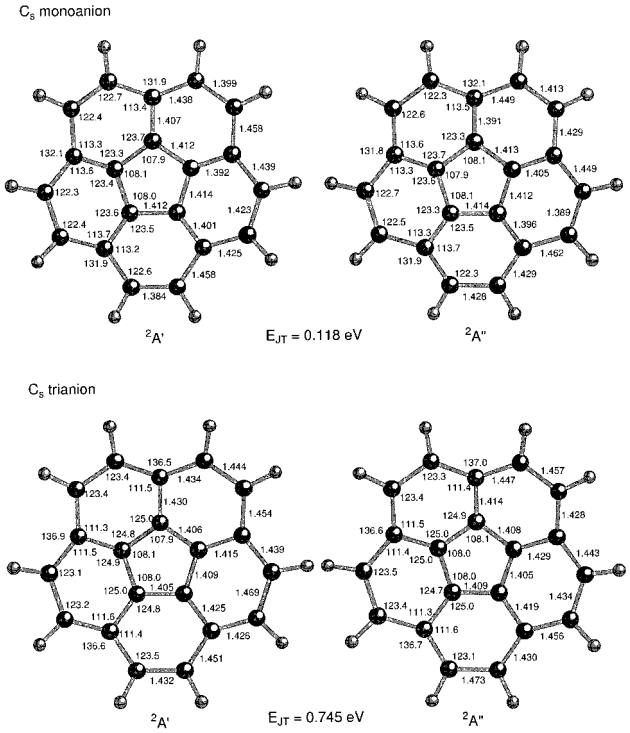

Figure 4. Optimized C_s structures of the mono- and trianions of corannulene.

reasonable in view of the LUMO. The bonds *n* and *m* in the ^{2}A′ state are increased and decreased, respectively, compared to the original one in the neutral state; in contrast the bonds *n* and *m* in the ^{2}A″ state are decreased and increased, respectively, compared to the original one in the neutral state. All of the hub bonds in the anions are decreased compared to those of the neutral state. This result is also reasonable. The phase patterns of the LUMO and the HOMO are very similar in the hub moiety, but the atomic orbitals between each spoke bond in the HOMO and the LUMO are combined in phase and out of phase, respectively. Because of the antibonding character seen in the LUMO with respect to the spoke bonds, they are stretched in these anions and as a consequence the inner five-membered ring can be compressed especially in the trianion to lead to the decrease in the hub bonds.

However, the distance changes in the hub bonds are much smaller than those in the rim bonds. This result may be explained by the so-called "an annulene within an annulene" concept.[1,7ab] According to this concept, it is possible to view the neutral corannulene as an aromatic 5C/6e hub suspended within an aromatic 15C/14e rim, the tetraanion as an aromatic 5C/6e hub suspended within an 15C/18e rim, and the mono-, di-, and trianions as species composed of aromatic 5C/6e hubs and 15C rims around which varying numbers of π electrons circulate, likewise concentric anions.[7b] Hence, the electron density in the hub moiety would not change significantly by electron doping compared to the electron density in the rim moiety. This can explain why the rim bonds are significantly increased while the hub bonds are not remarkably changed.

TABLE 3: Optimized C−C Bond Lengths of Corannulene and Its Mono- and Trianions; Values in Parentheses Are the Bond-Length Changes from the Values of Neutral Corannulene

		neutral (C_{5v})	monoanion (C_s)		trianion (C_s)	
		$^1A_1$	$^2A'$	$^2A''$	$^2A'$	$^2A''$
a			1.407 (+0.022)	1.391 (+0.006)	1.430 (+0.045)	1.414 (+0.029)
b	spoke	1.385	1.392 (+0.007)	1.405 (+0.020)	1.415 (+0.030)	1.429 (+0.044)
c			1.401 (+0.016)	1.396 (+0.011)	1.425 (+0.040)	1.419 (+0.034)
d			1.412 (−0.005)	1.413 (−0.004)	1.406 (−0.011)	1.408 (−0.009)
e	hub	1.417	1.414 (−0.003)	1.412 (−0.005)	1.409 (−0.008)	1.405 (−0.012)
f			1.412 (−0.005)	1.414 (−0.003)	1.405 (−0.012)	1.409 (−0.008)
g			1.399 (+0.009)	1.413 (+0.023)	1.444 (+0.054)	1.457 (+0.067)
h	rim	1.390	1.423 (+0.033)	1.389 (−0.001)	1.469 (+0.079)	1.434 (+0.044)
i			1.384 (−0.006)	1.428 (+0.038)	1.432 (+0.042)	1.473 (+0.083)
j			1.438 (−0.010)	1.449 (+0.001)	1.434 (−0.014)	1.447 (−0.001)
k			1.458 (+0.010)	1.429 (−0.019)	1.454 (+0.006)	1.428 (−0.020)
l	flank	1.448	1.439 (−0.009)	1.449 (+0.001)	1.439 (−0.009)	1.443 (−0.005)
m			1.425 (−0.023)	1.462 (+0.014)	1.426 (−0.022)	1.456 (+0.008)
n			1.458 (+0.010)	1.429 (−0.019)	1.451 (+0.003)	1.430 (−0.018)

TABLE 4: Calculated Vibrational Frequencies of the $^2A'$ and $^2A''$ States of the Monoanion with C_s Symmetry

$^2A'$	wavenumber (cm^{-1})
A′	129, 145, 275, 286, 405, 414, 434, 546, 558, 591, 600, 637, 643, 724, 745, 775, 792, 794, 842, 859, 906, 1034, 1092, 1125, 1154, 1207, 1221, 1264, 1331, 1382, 1433, 1452, 1466, 1476, 1495, 1599, 1632, 1649, 3126, 3128, 3148, 3150, 3154
A″	615i, 151, 288, 310, 400, 445, 458, 517, 549, 637, 645, 661, 672, 748, 766, 781, 797, 846, 862, 894, 932, 936, 1110, 1119, 1154, 1216, 1239, 1282, 1315, 1396, 1405, 1435, 1480, 1526, 1555, 1643, 3124, 3125, 3128, 3148, 3151

$^2A''$	wavenumber (cm^{-1})
A′	129, 145, 285, 311, 400, 433, 457, 546, 558, 591, 600, 643, 665, 724, 750, 767, 790, 794, 859, 874, 924, 1034, 1091, 1114, 1146, 1207, 1223, 1264, 1313, 1380, 1403, 1433, 1461, 1479, 1492, 1629, 1642, 1649, 3125, 3127, 3148, 3151, 3154
A″	616i, 151, 275, 288, 405, 413, 447, 516, 548, 634, 639, 645, 668, 744, 772, 782, 799, 833, 857, 869, 924, 936, 1110, 1136, 1157, 1215, 1239, 1283, 1331, 1398, 1434, 1467, 1475, 1526, 1555, 1599, 3124, 3126, 3128, 3148, 3150

Calculated relative bowl depths for the neutral, monoanionic, and trianionic states are 0.86, 0.80, and 0.51 Å, respectively. These results are in agreement with previous molecular orbital calculations on the monoanions and tetraanions,[8g] and we can state that the curvature of corannulene is decreased by electron doping. Of course, these interesting geometrical changes have relevance to the atomic motion in the E_2 modes of vibration that causes Jahn−Teller distortions in these anions. Calculated Jahn−Teller stabilization energies in the mono- and trianions are 0.12 and 0.75 eV, respectively, as indicated in Figure 4. These stabilization energies are larger than those in the coronene anions (0.08 and 0.42 eV in the mono- and trianions, respectively),[25] as expected.

We performed vibrational analyses for the $^2A'$ and the $^2A''$ states of the monoanion. Computed vibrational frequencies are listed in Table 4. One imaginary vibrational mode of A″ label is found for each optimized C_s structure, thus suggesting that the true energy-minimum structures for the corannulene monoanion should have no symmetry (C_1). This computational result is not in agreement with the prediction based on the epikernel principle[36] mentioned above; however, it is due to a consequence of higher-order effects that are not included within the framework of the first-order treatment. Because the energy gap between the SOMO and the LUMO in these monoanions is small (∼1 eV), we reasonably expect second-order Jahn−Teller distortions to take place. In fact, the symmetry label of the imaginary modes is consistent with the direct product of the A′ and the A″ states.

Corannulene and Coronene. It is useful to characterize the electronic and vibronic features of corannulene taking into account those of benzene, [18]annulene, [30]annulene, and coronene,[23−25] these being planar D_{6h} or D_{3h} aromatic hydrocarbons. In Figure 5 computed vibronic coupling constants in the trianions of these aromatic hydrocarbons are shown. We can derive three general conclusions from the previous papers:

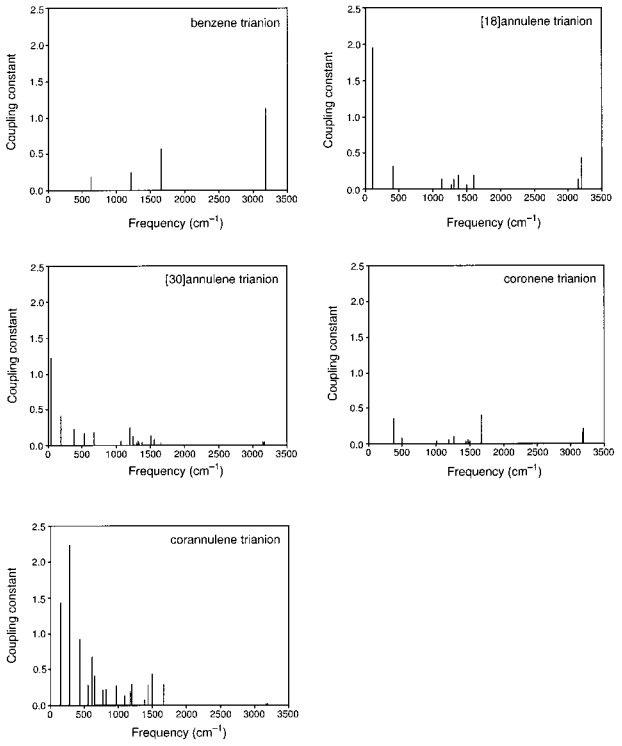

Figure 5. Vibronic coupling constants for the trianions of benzene, [18]annulene, [30]annulene, coronene, and corannulene. The values of vibronic coupling constants in benzene and [18]annulene are different from those in ref 23 by the factor of 2π.

(1) low-frequency modes in the higher annulenes have large vibronic coupling constants, thus playing an important role in their Jahn−Teller distortions; (2) in negatively charged coronene both low- and high-frequency modes are important for the Jahn−Teller distortions as if the electronic properties of benzene and

[18]annulene still remain in coronene; and (3) high-frequency modes in benzene give large coupling constants. We can now reconfirm these vibronic features in Figure 5. In negatively charged corannulene, the low-frequency modes of 142 cm^{-1} (ω_1) and 282 cm^{-1} (ω_2) play an important role in the Jahn−Teller distortions as mentioned above, and this feature is somewhat similar to that of [30]annulene. One may think that the vibronic interaction in the corannulene anions would be similar to that of the coronene anions; however, the structural difference between corannulene and coronene leads to a remarkable contrast in their vibronic interactions. Because in coronene the inner 6-membered ring is combined with the outer 18-membered ring through the six spoke bonds, the D_{6h} framework of coronene is rather rigid from the concept of an annulene within an annulene.[1,7ab] Although in corannulene there are spoke bonds that combine the inner 5-membered ring and the outer 15-membered ring, the C_{5v} framework of corannulene is not so rigid, as confirmed from the facts that the carbon framework of corannulene is easily inverted at room temperature[4b,8de] and the relative bowl depth is significantly decreased by electron doping.[8g] The Jahn−Teller active E_2 modes of vibration have relevance to the interesting molecular motion, as can be seen in Figure 3. On the other hand, the Jahn−Teller active E_{2g} modes of coronene and the resultant molecular distortions in its anions are strictly fixed on the molecular plane by symmetry.[25] We can thus conclude that the flexible Jahn−Teller E_2 modes coming from the bowl-shaped structure of corannulene should lead to large vibronic coupling constants. On the basis of these electronic and vibronic features of corannulene and coronene, we can predict that the electron−phonon coupling constants in the fullerene complexes should be larger than those in the GICs. This may be one of the reasons that the T_c values in the A_3C_{60} complexes are much higher than those in the GICs.

Conclusions

We computed and analyzed the vibrational frequencies, the vibronic coupling constants, and the Jahn−Teller distortions in the mono- and trianions of corannulene. First, we optimized the structure of neutral corannulene with C_{5v} symmetry at the level of B3LYP/6-31G*. The optimized structure is in good agreement with that determined from an X-ray analysis. Next, we performed a vibrational analysis in this optimized structure and confirmed that all frequency modes are real, suggesting that the optimized structure of the bowl-shaped form with C_{5v} symmetry is the energy minimum structure. Furthermore, we calculated the vibronic coupling constants for the mono- and trianions. The lowest two E_2 modes of 142 cm^{-1} (ω_1) and 282 cm^{-1} (ω_2) have large coupling constants in both anions, and we therefore expect these vibrational modes to greatly contribute to the Jahn−Teller distortions. The vibronic features in the corannulene anions are different from those in the coronene anions in that the coupling constants of the corannulene anions are much larger than those of the coronene anions. This difference should stem from the fact that corannulene has a bowl-shaped structure, whereas coronene does not. The atomic motion in the Jahn−Teller active E_2 modes of corannulene is somewhat vertical to the bowl-shaped structure. However, the Jahn−Teller active E_{2g} modes of coronene and the resultant molecular distortions in its anions are strictly fixed on the molecular plane by symmetry. From these points of view, we suggest that the electron−phonon coupling in the fullerene complexes should be stronger than that in the GICs. This may be one of the reasons that the T_c values of the A_3C_{60} complexes are higher than those of the GICs. Finally, we optimized the structure of the corannulene anions with C_s symmetry and calculated the Jahn−Teller stabilization energies. Calculated Jahn−Teller stabilization energies are 0.118 and 0.745 eV in the mono- and trianions, respectively, and these values are larger than those in the coronene anions. We found that the central hub bonds are not significantly changed by electron doping, whereas the peripheral rim bonds are stretched. These results can be explained in view of the phase patterns of the LUMO which is partially occupied in the mono- and trianions. We also reconfirmed that the curvature of corannulene is significantly decreased by electron doping.

Acknowledgment. This work was supported by the "Research for the Future" Program from the Japan Society for the Promotion of Science (JSPS-RFTF96P00206) and by a Grant-in-Aid for Scientific Research on the Priority Area "Carbon Alloys" from the Ministry of Education, Science, Sports and Culture of Japan. T.K. is grateful to the JSPS for a graduate fellowship. Computations were partly carried out at the Supercomputer Laboratory of Kyoto University and at the Computer Center of the Institute for Molecular Science.

References and Notes

(1) (a) Barth, W. E.; Lawton, R. G. *J. Am. Chem. Soc.* **1966**, *88*, 380. (b) Barth, W. E.; Lawton, R. G. *J. Am. Chem. Soc.* **1971**, *93*, 1730.

(2) Gleicher, G. J. *Tetrahedron* **1967**, *23*, 4257.

(3) Hanson, J. C.; Nordman, C. E. *Acta Crystallogr., Sect. B* **1976**, *B32*, 1147.

(4) (a) Scott, L. T.; Hashemi, M. M.; Meyer, D. T.; Warren, H. B. *J. Am. Chem. Soc.* **1991**, *113*, 7082. (b) Scott, L. T.; Hashemi, M. M.; Bratcher, M. S. *J. Am. Chem. Soc.* **1992**, *114*, 1920. (c) Borchardt, A.; Fuchicello, A.; Kilway, K. V.; Baldridge, K. K.; Siegel, J. S. *J. Am. Chem. Soc.* **1992**, *114*, 1921.

(5) Kroto, H. W.; Heath, J. R.; O'Brien, S. C.; Curl, R. F.; Smalley, R. E. *Nature* **1985**, *318*, 162.

(6) Krätschmer, W.; Lamb, L. D.; Fostiropoulos, K.; Huffman, D. R. *Nature* **1990**, *347*, 354.

(7) (a) Ayalon, A.; Rabinovitz, M.; Cheng, P.-C.; Scott, L. T. *Angew. Chem., Int. Ed. Engl.* **1992**, *31*, 1636. (b) Baumgarten, M.; Gherghel, L.; Wagner, M.; Weitz, A.; Rabinovitz, M.; Cheng, P.-C.; Scott, L. T. *J. Am. Chem. Soc.* **1995**, *117*, 6254. (c) Ayalon, A.; Sygula, A.; Cheng, P.-C.; Rabinovitz, M.; Rabideau, P. W.; Scott, L. T. *Science* **1994**, *265*, 1065.

(8) (a) Peck, R. C.; Schulman, J. M.; Disch, R. L. *J. Phys. Chem.* **1990**, *94*, 6637. (b) Abdourazak, A. H.; Sygula, A.; Rabideau, P. W. *J. Am. Chem. Soc.* **1993**, *115*, 3010. (c) Rabideau, P. W.; Marcinow, Z.; Sygula, R.; Sygula, A. *Tetrahedron Lett.* **1993**, *34*, 6351. (d) Disch, R. L.; Schulman, J. M. *J. Am. Chem. Soc.* **1994**, *116*, 1533. (e) Sygula, A.; Rabideau, P. W. *J. Chem. Soc., Chem. Commun.* **1994**, 1497. (f) Martin, J. M. L. *Chem. Phys. Lett.* **1996**, *262*, 97. (g) Tanaka, K.; Sato, T.; Okada, M.; Yamabe, T. *Fullerene Sci. Technol.* **1996**, *4*, 863.

(9) (a) Bakowies, D.; Thiel, W. *Chem. Phys.* **1991**, *151*, 309; *J. Am. Chem. Soc.* **1991**, *113*, 3704. (b) Cyvin, S. J.; Brendsdai, E.; Brunvoll, J.; Skaret, M. *THEOCHEM* **1991**, *247*, 119. (c) Matsuzawa, N.; Dixon, D. A. *J. Phys. Chem.* **1992**, *96*, 6241. (d) Sastry, G. N.; Jemmis, E. D.; Mehta, G.; Shah, S. R. *J. Chem. Soc., Perkin Trans.* **1993**, 1867. (e) Pope, C. J.; Howard, J. B. *J. Phys. Chem.* **1995**, *99*, 4306. (f) Chakrabarti, A.; Anusooya, Y.; Ramasesha, S. *THEOCHEM* **1996**, *361*, 181. (g) Yavari, I.; Taj-Khorshid, E.; Nori-Shargh, D.; Balalaie, S. *THEOCHEM* **1997**, *393*, 163.

(10) (a) Hebard, A. F.; Rosseinsky, M. J.; Haddon, R. C.; Murphy, D. W.; Glarum, S. H.; Palstra, T. T. M.; Ramirez, A. P.; Kortan, A. R. *Nature* **1991**, *350*, 600. (b) Rosseinsky, M. J.; Ramirez, A. P.; Glarum, S. H.; Murphy, D. W.; Haddon, R. C.; Hebard, A. F.; Palstra, T. T. M.; Kortan, A. R.; Zahurak, S. M.; Makhija, A. V. *Phys. Rev. Lett.* **1991**, *66*, 2830.

(11) Tanigaki, K.; Ebbesen, T. W.; Saito, S.; Mizuki, J.; Tsai, J. S.; Kubo, Y.; Kuroshima, S. *Nature* **1991**, *352*, 222.

(12) Palstra, T. T. M.; Zhou, O.; Iwasa, Y.; Sulewski, P. E.; Fleming, R. M.; Zegarski, B. R. *Solid State Commun.* **1995**, *93*, 327.

(13) Varma, C. M.; Zaanen, J.; Raghavachari, K. *Science* **1991**, *254*, 989.

(14) Lannoo, M.; Baraff, G. A.; Schluter, M.; Tomanek, D. *Phys. Rev. B* **1991**, *44*, 12106.

(15) (a) Asai, Y.; Kawaguchi, Y. *Phys. Rev. B* **1992**, *46*, 1265. (b) Faulhaber, J. C. R.; Ko, D. Y. K.; Briddon, P. R. *Phys. Rev. B* **1993**, *48*, 661. (c) Antropov, V. P.; Gunnarsson, O.; Liechtenstein, A. I. *Phys. Rev. B* **1993**, *48*, 7651. (d) Manini, N.; Tosatti, E.; Auerbach, A. *Phys. Rev. B*

1994, *49*, 13008. (e) Gunnarsson, O. *Phys. Rev. B* **1995**, *51*, 3493. (f) Tanaka, K.; Huang, Y.; Yamabe, T. *Phys. Rev. B* **1995**, *51*, 12715. (g) Dunn, J. L.; Bates, C. A. *Phys. Rev. B* **1995**, *52*, 5996.

(16) Jahn, H. A.; Teller, E. *Proc. R. Soc. London, Ser. A* **1937**, *161*, 220.

(17) Hannary, N. B.; Geballe, T. H.; Matthias, B. T.; Andress, K.; Schmidt, P.; MacNair, D. *Phys. Rev. Lett.* **1965**, *14*, 225.

(18) Belash, I. T.; Bronnikov, A. D.; Zharikov, O. V.; Palnichenko, A. V. *Synth. Met.* **1990**, *36*, 283.

(19) Avdeev, V. V.; Zharikov, O. V.; Nalimova, V. A.; Palnichenko, A. V.; Semenenko, K. N. *Pis'ma Zh. Eksp. Teor. Fiz.* **1986**, *43*, 376.

(20) Clarke, R.; Uher, C. *Adv. Phys.* **1984**, *33*, 469.

(21) Haddon, R. C. *Acc. Chem. Res.* **1992**, *25*, 127.

(22) Devos, A.; Lannoo, M. *Phys. Rev. B* **1998**, *58*, 8236.

(23) Yoshizawa, K.; Kato, T.; Yamabe, T. *J. Chem. Phys.* **1998**, *108*, 7637.

(24) (a) Kato, T.; Yoshizawa, K.; Yamabe, T. *Chem. Phys.* **1999**, *247*, 375. (b) Yoshizawa, K.; Tachibana, M.; Yamabe, T. *Bull. Chem. Soc. Jpn.* **1999**, *72*, 697.

(25) Kato, T.; Yoshizawa, K.; Yamabe, T. *J. Chem. Phys.* **1999**, *110*, 249.

(26) Yoshizawa, K.; Kato, T.; Yamabe, T. *J. Chem. Phys.* **1998**, *109*, 8514.

(27) Yoshizawa, K.; Kato, T.; Tachibana, M.; Yamabe, T. *J. Phys. Chem. A* **1998**, *102*, 10113.

(28) Yoshizawa, K.; Tachibana, M.; Yamabe, T. *J. Chem. Phys.* **1999**, *111*, 10088.

(29) (a) Bersuker, J. B. *The Jahn−Teller Effect and Vibronic Interactions in Modern Chemistry*; Plenum: New York, 1984. (b) Bersuker, J. B.; Polinger, V. Z. *Vibronic Interactions in Molecules and Crystals*; Springer: Berlin, 1989.

(30) Conwell, E. M. *Phys. Rev. B* **1980**, *22*, 1761.

(31) (a) Becke, A. D. *Phys. Rev. A* **1988**, *38*, 3098. (b) Becke, A. D. *J. Chem. Phys.* **1993**, *98*, 5648.

(32) Lee, C.; Yang, W.; Parr, R. G. *Phys. Rev. B* **1988**, *37*, 785.

(33) (a) Ditchfield, R.; Hehre, W. J.; Pople, J. A. *J. Chem. Phys.* **1971**, *54*, 724. (b) Hariharan, P. C.; Pople, J. A. *Theor. Chim. Acta* **1973**, *28*, 213.

(34) Frisch, M. J.; Trucks, G. W.; Schlegel, H. B.; Gill, W. P. M.; Johnson, B. G.; Robb, M. A.; Cheeseman, J. R.; Keith, T. A.; Patterson, G. A.; Montgomery, J. A.; Reghavachari, K.; Al-Laham, M. A.; Zakrzewski, V. G.; Ortiz, J. V.; Foresman, J. B.; Cioslowski, J.; Stefanov, B. B.; Nanayakkara, A.; Challacombe, M.; Peng, C. Y.; Ayala, P. Y.; Chen, W.; Wong, M. W.; Andres, J. L.; Replogle, E. S.; Gomperts, R.; Martin, R. L.; Fox, D. J.; Binkley, J. S.; Defrees, D. J.; Baker, J.; Stewart, J. J. P.; Head-Gordon, M.; Gonzalez, C.; Pople, J. A. *GAUSSIAN 94*; Gaussian Inc.: Pittsburgh, PA, 1995.

(35) (a) Hawkins, J. M.; Meyer, A.; Lewis, T. A.; Loren, S.; Hollander, F. J. *Science* **1991**, *252*, 312. (b) Fagan, P. J.; Calabrese, J. C.; Malone, B. *Science* **1991**, *252*, 1160.

(36) Ceulemans, A.; Vanquickenborne, L. G. *Structure and Bonding*; Springer: Berlin, 1989; Vol. 71.